JOURNAL OF BACTERIOLOGY, May 1996, p. 2825–2835 Vol. 178, No. 10
0021-9193/96/$04.00+0

Surveying a Supercoil Domain by Using the γδ Resolution System in *Salmonella typhimurium*

N. PATRICK HIGGINS,[1]* XIANGLI YANG,[1] QINGQUAN FU,[1] AND JOHN R. ROTH[2]

Department of Biochemistry, University of Alabama at Birmingham, Birmingham, Alabama 35294-2170,[1] *and Department of Biology, University of Utah, Salt Lake City, Utah 84112*

Received 30 October 1995/Accepted 6 March 1996

A genetic system was developed to investigate the supercoil structure of bacterial chromosomes. New *res*-carrying transposons were derived from Mu*d*I1734 (Mu*d*Jr1 and Mu*d*Jr2) and Tn*10* (Tn*10d*Gn). The Mu*d*Jr1 and Mu*d*Jr2 elements each have a *res* site in opposite orientation so that when paired with a Tn*10d*Gn element in the same chromosome, one Mu*d*Jr *res* site will be ordered as a direct repeat. Deletion formation was studied in a nonessential region (~100 kb) that extends from the *his* operon through the *cob* operon. Strains with a Mu*d*Jr insertion in the *cobT* gene at the 5′ end of the *cob* operon plus a Tn*10d*Gn insertion positioned either clockwise or counterclockwise from *cobT* were exposed to a burst of RES protein. Following a pulse of resolvase expression, deletion formation was monitored by scoring the loss of the Lac^+ phenotype or by loss of tetracycline resistance. In exponentially growing populations, deletion products appeared quickly in some cells (in 10 min) but also occurred more than an hour after RES induction. The frequency of deletion (y) diminished with increasing distance (x) between *res* sites. Results from 15 deletion intervals fit the exponential equation $y = 120 \cdot 10^{(-0.02x)}$. We found that *res* sites can be plectonemically interwound over long distances (>100 kb) and that barriers to supercoil diffusion are placed stochastically within the 43- to 45-min region of the chromosome.

DNA topology is important in many genetic processes. Negative supercoiling stimulates homologous recombination and is critical for a plethora of site-specific recombination systems that cause insertion, inversion, and deletion of DNA (20). One of the best studied site-specific recombination systems is contained within the γδ transposon (30, 51). Transposition of γδ from one chromosome to another occurs by a two-step process. First, a replicative transposition reaction creates a fusion (or cointegration) of the two chromosomes, which are joined by two copies of the γδ element ordered as direct repeats (30, 57). Second, the two γδ elements recombine to separate the two initial chromosomes, leaving each with a copy of γδ. This reciprocal site-specific resolution reaction requires a site in the element (the *res* sequence) and is catalyzed by the *tnpR* gene product (RES). The RES protein interacts with the *res* sequence both as a recombinase and as a repressor that regulates its own expression and that of γδ transposase. Therefore, the *res* sequence serves both as a recombination site and as a transcriptional operator site.

The site-specific recombination reaction described above has been characterized extensively in vitro and in vivo. The reaction proceeds efficiently without cofactors; it requires only supercoiled DNA and a single protein, RES. A cocrystal of the enzyme-DNA complex provides a model for studying the chemistry of recombination (54); the DNA substrate and products of resolution have been defined topologically with high precision (7, 8, 12, 20). The recombination substrate is a plectonemically tangled pair of *res* sites with three superhelical nodes (7, 10, 64). This geometric arrangement forms naturally on a single negatively supercoiled DNA substrate that includes two direct-order *res* sites. During the DNA strand exchange reaction, two supercoiled nodes are eliminated and the products are two singly linked circular DNA molecules.

* Corresponding author. Phone: (205) 934-3299. Fax: (205) 975-5955. Electronic mail address: nphiggins@bmg.bhs.uab.edu.

The rigorous topological requirements for resolution reactions provide an opportunity to study chromosome behavior in vivo. Inducing expression of RES protein initiates efficient recombination between *res* sites cloned on plasmids (10, 51) or between *res* sites engineered to flank a tetracycline resistance reporter gene in a bacterial chromosome (13). This resolution reaction has not been systematically applied to studies of the bacterial chromosome.

We wish to address the question of how an individual circular chromosome is arranged within the cell. Previous results suggest that the chromosome includes 50 to 100 independently supercoiled domains (33, 59). These domains could be fixed regions whose extent is determined by specific binding sites at a loop base, similar to models proposed for eucaryotic chromosomes (28, 29). Alternatively, domains could be highly plastic, with barriers being determined by transcriptional activity (27, 37) or by DNA gyrase binding sites (43, 44, 63). To decide such questions, we have constructed an assay system that uses RES protein (of transposon γδ) to form deletions between specific direct-order *res* sequences placed in the chromosome. A resolution reaction requires that the two *res* sites be localized in the same plectonemically tangled, supercoiled domain. We find that the rate of deletion formation decreases with the log of the distance between *res* sites, which suggests a stochastic arrangement for plectonemic supercoiling in the 43- to 45-min region of the chromosome. Rates of deletion formation also increase in stationary-phase cells, demonstrating physiological control over long-range DNA interactions.

MATERIALS AND METHODS

Bacterial strains and plasmids. Genotypes of the bacterial strains used in this work (all derivatives of *Salmonella typhimurium* LT2) are listed in Table 1. Plasmid pJBRESc**I** is a pACYC184-derived vector carrying the *tnpR* (RES protein) gene of transposon γδ cloned under control of the λ p_L promoter with a nearby copy of λ *c*Its repressor gene (11). A plasmid containing the new transposon Tn*10d*Gn, which is derived from pNK373 (6, 25, 41), and plasmids for construction of Mu*d*Jr1 and Mu*d*Jr2 are shown in Fig. 1. The Tn*10d*Gn construct is a transposition-defective derivative of Tn*10* (69). The Tn*10* transposase gene

TABLE 1. Strains used[a]

Strain	Genotype	Plasmid
NH2000	*cobT62*::Mu*dJ*	pPH619
NH2009	*cobT62*::Mu*dJ*	
NH2021	*polA2 ara-9 cobT62*::Mu*dJ cobT*::pPH619	pPH619
NH2036	*polA2 ara-9 cobT62*::Mu*dJ cobT*::pPH619 *zea-3777*::Tn*10d*Tc	pPH619
NH2037	*polA2 ara-9 cobT62*::Mu*dJ*	
NH2041	*polA2 ara-9 cobT62*::Mu*dJ zea-3777*::Tn*10d*Tc	
NH2044	*cobT62*::Mu*dJ mutL*::Cm	
NH2048	*proA36 strA1*	F′::Tn*10d*Gn
NH2050	Wild-type strain LT2	pJBRES*c*I
NH2051	*cobT714*::Mu*dJ*r1 *zea-3777*::Tn*10d*Tc	pJBRES*c*I
NH2068	*polA2 ara9 cobT62*::Mu*dJ cobT*::pPH618 *zea-3777*::Tn*10d*Tc	pPH618
NH2075	*cobT714*::Mu*dJ*r1 *zea-3777*::Tn*10d*Tc *pduF358*::Tn*10d*Gn	pJBRES*c*I
NH2116	*cobT714*::Mu*dJ*r2 *zea-3777*::Tn*10d*Tc	pJBRES*c*I
NH2118	*cobT714*::Mu*dJ*r2 *zea-3777*::Tn*10d*Tc *cobP712*::Tn*10d*Gn	pJBRES*c*I
NH2119	*cobT714*::Mu*dJ*r2 *zea-3777*::Tn*10d*Tc *cob-708*::Tn*10d*Gn	pJBRES*c*I
NH2123	*cobT714*::Mu*dJ*r2 *zea-3777*::Tn*10d*Tc *zea-3786*::Tn*10d*Gn	pJBRES*c*I
NH2124	*cobT714*::Mu*dJ*r2 *zea-3777*::Tn*10d*Tc *cobU713*::Tn*10d*Gn	pJBRES*c*I
NH2130	*cobΔ15* (*cob-708*::Tn*10d*Gn-*cobT714*::Mu*dJ*r2)	pJBRES*c*I
NH2140	*cobT714*::Mu*dJ*r1 *zea-3777*::Tn*10d*Tc *cobP710*::Tn*10d*Gn	pJBRES*c*I
NH2141	*cobT714*::Mu*dJ*r1 *zea-3777*::Tn*10d*Tc *zea-3787*::Tn*10d*Gn	pJBRES*c*I
NH2142	*cobT714*::Mu*dJ*r1 *zea-3777*::Tn*10d*Tc *cobJ709*::Tn*10d*Gn	pJBRES*c*I
NH2149	*cobT714*::Mu*dJ*r2 *zea-3777*::Tn*10d*Tc *hisD10201*:Tn*10d*Gn	pJBRES*c*I
NH2172	*cobT714*::Mu*dJ*r1 *zea-3777*::Tn*10d*Tc *pduC359*::Tn*10d*Gn	pJBRES*c*I
NH2223	*cobT714*::Mu*dJ*r2 *zea-3777*::Tn*10d*Tc *phs-208*::Tn*10d*Gn	pJBRES*c*I
NH2226	*cobT714*::Mu*dJ*r1 *zea-3777*::Tn*10d*Tc *zee-8251*::Tn*10d*Gn	pJBRES*c*I
NH2369	*cobT714*::Mu*dJ*r2 *zea-3777*::Tn*10d*Tc *pdu-360*::Tn*10d*Gn	pJBRES*c*I
NH2370	*cobT714*::Mu*dJ*r1 *zea-3777*::Tn*10d*Tc *pdu-361*::Tn*10d*Gn	pJBRES*c*I
NH2453	*cobT714*::Mu*dJ*r2 *zea-3777*::Tn*10d*Tc *zec-8253*::Tn*10d*Gn	pJBRES*c*I
TT10427	Wild-type strain LT2	pNK972

[a] All strains were derived from *S. typhimurium* LT2, and all except TT10427 (Roth Collection) were constructed during this work.

of IS*10*L on this plasmid is expressed under control of a p_{tac} (IPTG [isopropyl-β-D-thiogalactopyranoside]-inducible) promoter. Details on construction are available on request.

Genetic techniques. Transductional crosses were carried out as described previously (22) with P22 HT 105/1 *int-201*, a high-efficiency transducing mutant of bacteriophage P22 (56). For transductional crosses involving selection for resistance to chloramphenicol (Cm^r), ampicillin (Ap^r), tetracycline (Tc^r), or kanamycin (Kn^r), phages and recipient cells were mixed and incubated at 37°C for 45 min before spreading onto selective plates. For transductional crosses involving resistance to gentamicin (Gn^r), phages were incubated with recipient cells for 15 min at room temperature, and then EGTA [ethylene glycol-bis(β-aminoethyl ether)-*N*,*N*,*N*′,*N*′-tetraacetic acid] was added to a final concentration of 10 mM to stop further phage adsorption, and suspensions were incubated in a 37°C shaking incubator for at least 3 h before the cells were spread on selective medium. This extended incubation was needed to allow gentamicin acetyltransferase expression prior to exposure to selective conditions. Phage-free transductants were isolated by streaking nonselectively on green indicator plates (62). To check for phage sensitivity, strains were cross-streaked with a clear plaque mutant of P22 (22).

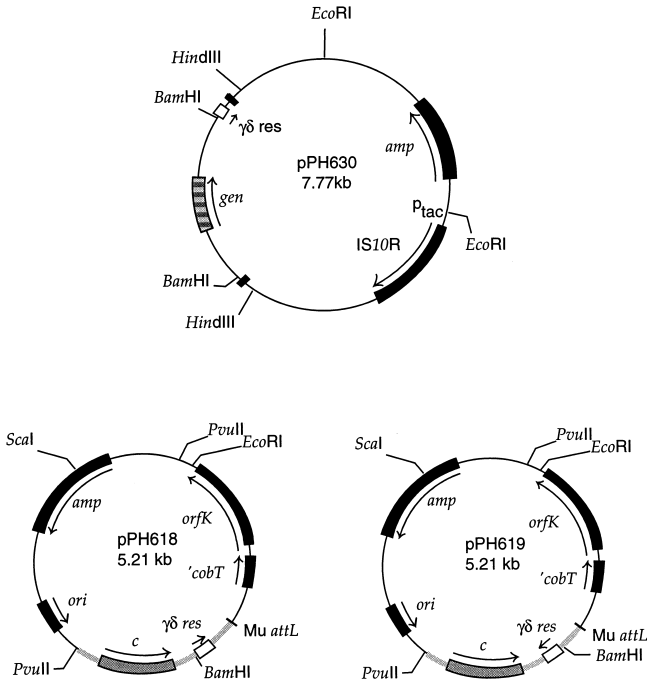

FIG. 1. Diagram of plasmids constructed for this work.

Media. Complex medium was LB medium (10 g of NaCl, 10 g of tryptone, 5 g of yeast extract per liter). Minimal media were based on NCE salts (E medium without citrate) described previously (9, 22); either 0.2% glucose or 1% sodium succinate was added as a carbon source. For phenotypic scoring of *pdu* (propanediol utilization) mutants, cells were plated on MacConkey-propanediol-vitamin B_{12} medium and incubated in an anaerobic chamber (BBL GasPak Plus; Becton Dickinson). For phenotypic analyses of *phs* (production of H_2S) mutants, cells were stabbed into Kligler iron agar (Difco) as suggested by Voll et al. (67). The following nutritional supplements were added to the final concentrations indicated: amino acids, 0.5 mM; cobinamide dicyanide, 16 μg/liter; 5,6-dimethylbenzimidazole, 44 μg/liter. Antibiotics were added to LB medium at concentrations of 50 μg/ml for kanamycin and ampicillin, 20 μg/ml for chloramphenicol, 20 μg/ml for tetracycline, and 10 μg/ml for gentamicin (unless stipulated otherwise). Antibiotics were added to NCE-based media at concentrations of 125 μg/ml for kanamycin, 50 μg/ml for ampicillin, 10 μg/ml for tetracycline, 10 μg/ml for gentamicin (unless stipulated otherwise), and 5 μg/ml for chloramphenicol.

PCRs. Short-range PCRs were done with the recombinant Ampli*Taq* polymerase from Perkin-Elmer and the thermocycling conditions, times, and buffers recommended by the manufacturer of the model 1605 air thermocycler (Idaho Technology). Long-range PCRs were performed by the method described by Cheng et al. (17). Oligonucleotides used for diagnosing the chromosomal insertion products include the following: 161OU**I**, which matches a segment of *cobT*, positions 968 to 948 (GenBank accession number L3547); Res6, which matches the reverse complement of bp 2899 to 2879 of Tn*1000* (accession number X60200); GP1, which matches Tn*1696* bp 2278 to 2299 (71); GP2, which matches

TABLE 2. Characterization of Tn*10d*Gn mutants

Allele	Affected gene	Diagnostic primer pairs	PCR band size (kb)	Transductional linkage	Compatible Mu*d*Jr
zea-3786	ND[a]	Res6 + 1610BB**I**	3.8[b]	96% to *cobT*	Mu*d*Jr2
zea-3787	ND	GP1 + 161OU**II**	8[b]	24% to *cobT*	Mu*d*Jr1
cob-708	None[c]	GP3 + VBP2F	1.1	55% to *cobT*	Mu*d*Jr2
cobJ709	*cobJ*	GP1 + MuR	5.5[b]	47% to *cobT*	Mu*d*Jr1
cobP710	*cobP*	GP3 + MuR	1.5	96% to *cobT*	Mu*d*Jr1
cobP712	*cobP*	GP1 + MuR	1.5	83% to *cobT*	Mu*d*Jr2
cobU713	*cobU*	GP1 + MuR	0.6	95% to *cobT*	Mu*d*Jr2
pduF358	*pduF*	GP1 + TB27	2.5	25% to *cobT*	Mu*d*Jr1
pduC359	*pduC*	GP2 + TB39	1.5	90% to *cobF*	Mu*d*Jr1
pdu-360	ND	GP3 + TB28	2.2	86% to *cobF*	Mu*d*Jr1
pdu-361	ND	GP2 + TB28	8[b]	55% to *cobF*	Mu*d*Jr1
zec-8253	ND[d]	ND	ND	72% to *hisD*	Mu*d*Jr2
phs-208	ND	GP2 + HF5	13[b]	78% to *hisD*	Mu*d*Jr2
hisD10201	*hisD*	ND	ND	95% to *hisD*	Mu*d*Jr1
zee-8251	ND	ND	ND	70% to *hisD*	Mu*d*Jr2

[a] ND, not determined.
[b] Insertion points determined by long-range PCRs (17).
[c] The *cob-708* insertion was found to be located within the *cob* transcript but upstream of the *cobA* initiation codon.
[d] This mutation was not detected by PCR, but it lies between the *phs* and *pdu* operons because deletions that form with this insertion and Mu*d*Jr2 are Cob$^-$ Pdu$^-$ Phs$^+$ His$^+$.

the reverse complement of Tn*1969* from bp 768 to 749; GP3, which matches the reverse complement of Tn*1696* from bp 849 to 830 (71); VBP2F, which matches bp 287 to 306 of the *pocR* gene (accession number L12006); MuR, which matches positions 23 to 47 of the Mu right end (and the *lacZ* end of a Mu*d* element) (68); 161OU**II**, which matches positions 1790 to 1807 in the *orfK* gene adjacent to *cobT* (16); TB27, which matches a 21-bp sequence in the *pduC* gene (11a); TB28 and TB39, which match 21-bp sequences in the *pduG* gene (11a); 1610BB**I**, which matches bp 1145 to 1162 in the noncoding region between the *cobT* and *ofrK* genes (16); and HF5, which matches bp 6948 to 6969 of the *hisG* gene (accession number X13464).

Tn*10* mutaagenesis. Tn*10d*Gn insertion mutants were isolated by transducing a copy of the element into recipient strain TT10427, which harbors Tn*10* transposase-producing plasmid pNK972 (25). The donor strain, NH2048, has a Tn*10d*Gn element in the F′ 128 *pro*$^+$ *lac*$^+$ plasmid. Gentamicin-resistant transductants from this cross cannot form by homologous recombination because the *Escherichia coli* DNA flanking the donor Tn*10d*Gn element is unique to the F′ plasmid in NH2048. Following phage infection and phenotypic expression, cells were spread on gentamicin-containing plates. A pool of 50,000 transductants made from 20 plates, each having 2,000 to 3,000 tiny gentamicin-resistant colonies, was suspended in 10 ml of 1× E salts (22) containing 10 mM EGTA, concentrated by centrifugation, and resuspended in 5 ml of 1× E salts with 10 mM EGTA. One milliliter of this cell suspension was diluted 20-fold into LB medium containing 10 mM EGTA plus 10 μg of gentamicin per ml, and a shaking culture was grown overnight. Cells from the overnight culture were harvested by centrifugation, suspended in an equal volume of 1× E salts, washed two times in 1× E salts, and then diluted 1:5 in LB medium containing 10^6 PFU of P22 phage per ml. After 8 h of incubation, the uninfected cells and debris were removed by centrifugation, and the phage-containing supernatant was stored over 0.5 ml of chloroform.

To isolate Tn*10d*Gn insertions with auxotrophic phenotypes, strain NH2009 was infected with phage grown on the pool of Tn*10d*Gn transposition mutants. After 3 h of incubation to allow expression of the gentamicin acetyltransferase, cells were spread onto LB medium-gentamicin plates. Auxotrophs, which were identified by replica plating to NCE salts-glucose plates containing 30 μg of gentamicin per ml, appeared at a frequency of about 1% of the Gn^r colonies and had growth requirements that were satisfied by the following nutritional additives: cysteine was required by nine colonies isolated; isoleucine was required by four; uracil was required by six; threonine was required by two; diaminopimelic acid was required by one; histidine was required by two; and additives were unidentified for five colonies. This distribution and frequency are similar to results reported for mutants generated by Tn*10d*Cm mutagenesis (25).

Mapping mutants in the 43- to 45-min region of *S. typhimurium*. In addition to auxotrophs, Tn*10d*Gn insertions linked to the *cob* region were isolated. In crosses involving phage donors grown on the pool of Tn*10d*Gn elements and recipient strain NH2009, mutants with a white colony phenotype appeared on X-Gal (5-bromo-4-chloro-3-indolyl-β-D-galactopyranoside) plates at a frequency of about 1 in 500 Gn^r colonies. Most of these were phenotypically Kn^s and had lost the *cobT*::Mu*d*J. In crosses involving Tn*10d*Gn elements near *cobT*, the recipient *cobT62*::Mu*d*J insertion was frequently replaced by a wild-type allele coinherited with the linked Tn*10d*Gn insertion.

Each Tn*10d*Gn insertion mutant near the *cobT62*::Mu*d*J insertion was tested for propanediol utilization and cobalamin synthesis, and transductional linkage to *cobT62*::Mu*d*J was measured. In most cases, these steps were sufficient to localize the insertions as being clockwise (near *supD*) or counterclockwise (near *his*) of the parental *cobT* insertion. Clockwise insertions (*zea-3786* and *zea-3787*) had no nutritional phenotype, whereas most counterclockwise insertions had either *cob* or *pdu* phenotypes. Second, to precisely locate the insertion points, oligonucleotide primers matching known positions in the *cob* and *pdu* operons (16, 52) were used in combination with oligonucleotides matching sequences within Tn*10d*Gn to generate PCR products. From the sizes of these PCR bands, the insertion points could be pinpointed. The diagnostic primer pairs and the PCR band sizes that were used to locate each mutant are given in Table 2. Five insertions in the *cob* operon were also subjected to DNA sequence analysis. Relative to the published sequence of the *cob* operon (GenBank accession number L12006), the following mutants were found: in the noncoding region upstream of the *cobA* gene at bp 1163, *cob-708*::Tn*10d*Gn; in *cobJ* at bp 9,313, *cobJ709*::Tn*10d*Gn; in *cobP* at bp 15,156, *cobP710*::Tn*10d*Gn; in *cobP* at bp 15,156, *cobP712*::Tn*10d*Gn, which is in the same site but opposite orientation relative to *cob-710*; and in *cobU* at bp 16,541, *cobU713*::Tn*10d*Gn.

Several Tn*10d*Gn insertion mutants were isolated that were not linked to the *cob* region by P22 transductional mapping but that could be placed in the vicinity of the *cob* operon by virtue of their phenotypic behavior or linkage to other markers. One insertion (*hisD10201*::Tn*10d*Gn) had a histidine requirement that was not satisfied by histidinol, which restricts the mutation to the *hisD* gene. Another mutant (*phs-208*::Tn*10d*Gn) was negative for hydrogen sulfide production and was found to be 78% linked by P22 transductional crosses to *hisD9952*::Mu*d*A. Two other mutants (*zee-8251* and *zec-8253*) were linked to the *his* operon (see Fig. 4). Several *pdu* mutants were isolated by virtue of their linkage to a blue Mu*d*J element in the *pduF* gene.

Molecular replacements for Mu*d*Jr1 and Mu*d*Jr2. The Mu*d*Jr1 and -2 elements (Fig. 2) are transposition-defective derivatives of Mu*d*I used for making operon fusions (14, 15). The strategy for constructing the Mu*d*Jr1 and -2 elements involved chromosomal replacement of segments in plasmids pPH618 and pPH619 (Fig. 2). Recombination of the *res* site modules in these plasmids into the chromosome requires two crossovers between the plasmid and chromosome, one in the Mu*d*J *c* repressor gene (labeled 1 in Fig. 2) and a second within the *cobT* segment (labeled 2 in Fig. 2). These recombination events were done in sequential transductional crosses. First, plasmid pPH619 was recombined into the chromosome by use of a transductional cross involving donor phage grown on strain NH2000, which carries plasmid pPH619, and recipient strain NH2037, which carries a *polA2* mutation. Because plasmid pPH619 has a ColE1-derived replication origin, stable inheritance of its *amp* gene required integration of the plasmid into the *S. typhimurium* chromosome by use of homology in the plasmid. These transductants were shown to carry the *amp* marker at a chromosomal site linked to the *cobT62*::Mu*d*J insertion.

The second step involved transduction of the chromosomally integrated copy of plasmid pPH691 to a *polA*$^+$ strain, screening for segregants that had lost plasmid sequences (i.e., that were Ap^s). Among these recombinants, we hoped to find one that retained the *res* site within the chromosomal Mu*d*J element (Fig. 2). This recombinant must use the homology patch (during plasmid excision in the *polA*$^+$ strain) that is different from that used for the initial integration step. Transductional crosses were done many times without recovering the desired recombinant. One reason for the failure of this experiment was a strong bias favoring recombination in the *cobT* homology patch (data not shown). We

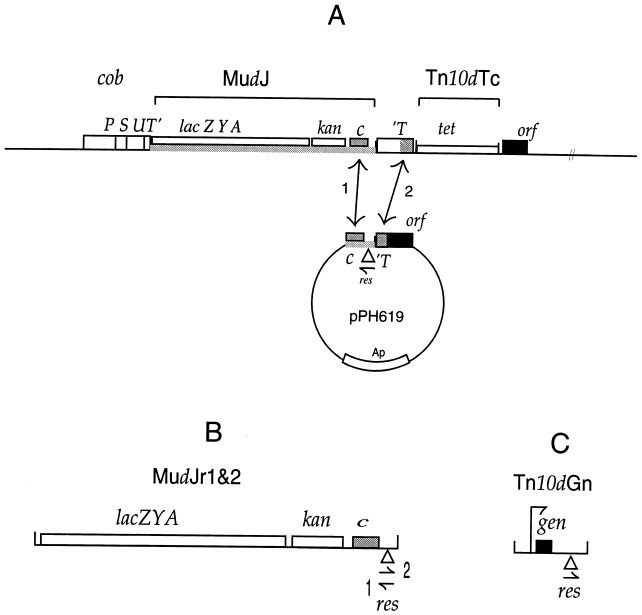

FIG. 2. Construction strategy for Mu*d*Jr2 and genetic maps of Mu*d*Jr1 and Mu*d*Jr2 and Tn*10d*Gn. (A) The genetic map of the 5′ end of the *cob* operon is shown with Mu*d*-derived sequences depicted as a thick gray line. Plasmid pPH619 is shown with the *res* site indicated by the triangle with underlying arrow. The desired recombination product (Materials and Methods) involved reciprocal exchanges at two positions indicated by arrows. To construct a Mu*d*Jr element, a reciprocal exchange must occur in the Mu *c* repressor gene (position 1) and a second must occur within a C-terminal fragment of the *cobT* gene (position 2). Recombinational methods are described in Results. (B) Genetic map of Mu*d*Jr1 and -2 elements, which include a promoterless *lac* operon, the neomycin phosphotransferase gene of Tn*903* (*kan*), the Mu *c* repressor gene, and the γδ *res* site in one of two orientations. (C) Genetic map of Tn*10d*Gn showing the location of the promoter and gentamicin acetyltransferase from Tn*1696* and the γδ *res* site.

overcame the bias by using a *mutL*::Cm allele in the transductional recipient (NH2044). Transductional crosses using phage stocks grown on NH2036 gave *res*-carrying substitutions in about 50% of the Ap^s transductants when NH2044 (*mutL*::Cm) was the recipient and gave fewer than 1 in 50 *res*-carrying substitutions when an isogenic *mut*$^+$ strain was the recipient. We do not understand the reason why the *mutL* pathway biases recombination so that a great preponderance of crossovers occur by use of the homology in *cobT*. Nevertheless, similar results were obtained with plasmid pPH618.

RESULTS

Using *res* sites to analyze chromosome structure in vivo—the basic strategy. The bacterial chromosome is thought to have independent supercoil domains, with DNA being interwound into branched loops (Fig. 3). It is not clear whether supercoil domains are fixed with clamps at specific sequences (Fig. 3) or whether the domains are dynamic with stochastically distributed end points, possibly subject to variation. The placement of nodes (the ends of long branches) might be directed by high-affinity gyrase sites (Fig. 3A) as points at which supercoils are persistently introduced (43). The methods developed here provide a way to investigate such questions in vivo.

If two *res* sites are located in the chromosome in direct order, they can recombine (in the presence of resolvase) to form a deletion. Previous work from several laboratories shows that this process requires the *res* sites to be on the same supercoiled DNA molecule such that they can become tangled together in a plectosome (11, 21, 64). In Fig. 3, the numbered circles represent *res* sites. The sites that can pair (i.e., sites 1 and 2 and sites 3 and 4) are expected to form a deletion, while sites in different supercoil domains (sites 1 and 3 or 4 and sites 2 and 3 or 4) that cannot be easily interwound and paired are not expected to form deletions. For sites spaced far apart in a chromosome to adopt the interwound alignment, one DNA strand must move by branching or slithering relative to its plectonemic partner (Fig. 3B). In testing these expectations, one must study a region in which the relevant deletion mutants are viable and can be recovered for analysis.

We constructed strains with *res*-carrying transposable elements (Tn*10* and Mu*d*) placed at positions that span about 100 kb of DNA in the 43- to 45-min segment of the *S. typhimurium* chromosome. This region is nonessential; deletions of the entire region or any portion can form without lethal consequences. Construction of *res*-bearing elements is described in Materials and Methods. The genetic and physical map (35a) of the chromosomal segment lying between the *his* and *cob* operons is shown with the locations of Tn*10d*Gn insertions in Fig. 4.

The assay system. An ideal assay for in vivo chromosome supercoiling behavior would meet three criteria. First, it should be possible to perform the assay at many different points in the chromosome. Second, the assay should be one that can be

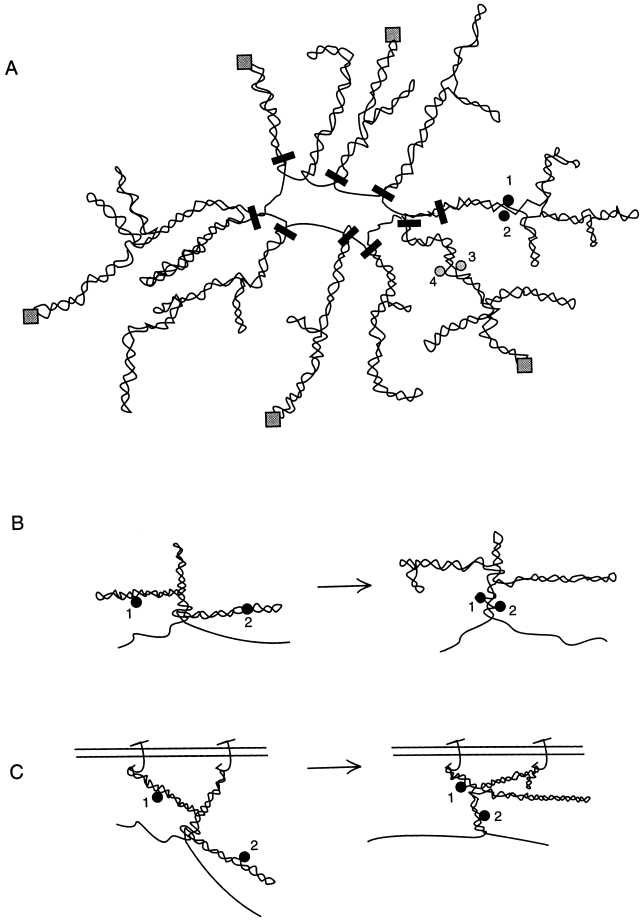

FIG. 3. Model of the interwound supercoiled bacterial chromosome. (A) Possible structural elements of chromosome organization suggested by in vitro and in vivo experiments (33, 34, 59) include supercoiling domain boundaries locked off by clamps (solid rectangles), and high-affinity gyrase binding sites (43) (shaded squares). Possibilities for pairing between different *res* sites (shown as numbered circles) are indicated (sites 1 and 2 and sites 3 and 4). (B) Movement of plectonemic supercoiling allowing two distant sites to become interwound together. (C) Example of how anchoring of DNA to a membrane, which is shown as hooks inserted into a lipid bilayer indicated as parallel lines, might limit supercoil movement.

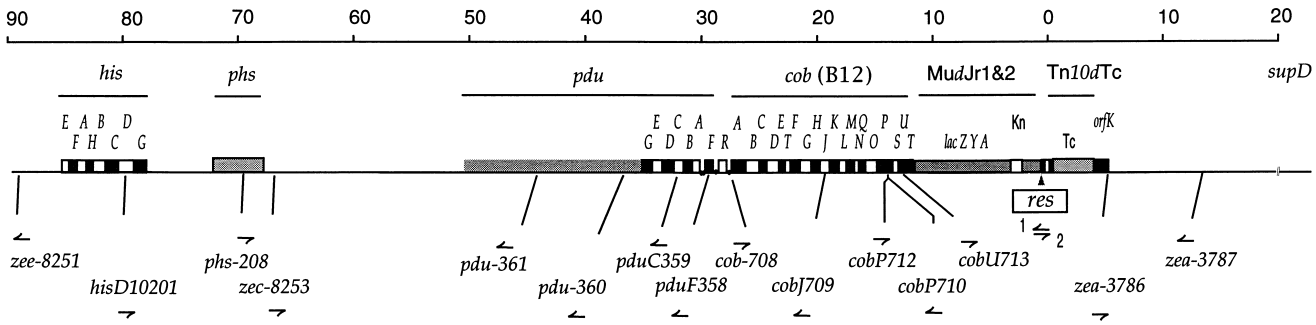

FIG. 4. Genetic and physical map of the 43- to 45-min region of *S. typhimurium*. The positions and orientations of the *his* operon (open boxes), *pdu* operon (shaded boxes), *cob* operon (white boxes), Mu*d*Jr2 (thick gray line), and *zea-3777*::Tn*10d*Tc (solid box) are shown along with the insertion points of different Tn*10d*Gn elements used in this work. The relative distances from the *res* site in Mu*d*Jr1 and Mu*d*Jr2 are shown above the map.

performed on cells growing under various conditions. Cell physiology might have a significant impact on chromosomal supercoiling. Third, the assay should be reproducible. Lack of reproducibility would weaken conclusions about the underlying organizational characteristics of the chromosome region under examination. We constructed strains to find out how well the γδ resolution system satisifies the three conditions listed above.

The basic procedure is to construct a series of strains each with *res* sequences at a pair of separated sites. The ability of a site to become locally interwound (plectonemically tangled) is measured by the deletion frequency following a pulse of RES expression. All strains had one *res* sequence in a Mu*d*J element inserted in the *cobT* gene. The second *res* site was present in a Tn*10d*Gn introduced either to the left or to the right of the *cobT* gene. The largest interval tested was 90 kb (between *cobT714*::Mu*d*Jr1 and *zee-8251*::Tn*10d*Gn), and the smallest interval tested was 6 kb (between *cobT714*::Mu*d*Jr2 and *zea-3786*::Tn*10d*Gn). All Tn*10d*Gn elements tested made deletions when paired with either Mu*d*Jr1 or -2 and exposed to a burst of γδ RES protein (Table 3). Thus, the first criterion for a useful supercoiling assay was met. We can analyze chromosome pairing interactions between many reference points.

Second, conditions were sought to generate a dose of resolvase that gives reproducible deletion efficiencies. Prolonged expression of resolvase (induction for an hour or more) was toxic and caused cultures to stop growth. A 10-min shift from 30 to 42°C followed by a shift back to 30°C with continued incubation in broth for 1 h stimulated sufficient RES synthesis in exponentially growing cells (as well as in stationary-phase cells) to stimulate efficient deletion of DNA between two direct-ordered *res* sites on a plasmid (reference 11 and data not shown). Control over the expression of RES protein in this heat-inducible system was tight but not absolute. As is the case for many genes cloned on multicopy plasmids, some expression of RES occurred at 30°C; rare white colonies were found among the cells of several uninduced cultures (Table 3). For example, the 12-kb deletion between *cobT714*::Mu*d*Jr2 and *cobU713*::Tn*10d*Gn in NH2124 was found in less than 1% of the colonies without heat induction (Fig. 4; Table 3). However, even these deletions were RES dependent, since they were not found in cells lacking plasmid pJBRES*c*I (data not shown). The background deletion formation in uninduced cells with the RES plasmid was low enough that it did not hamper measurements; induced cultures of cells in the exponential phase of growth or in the stationary phase gave at least 30-fold increases

TABLE 3. Characterization of deletion products in exponential-phase cells

Strain	Allele	Deletion size (kb)	Uninduced deletion frequency (%)	Induced deletion frequency (% [mean ± SD])	% of deletions with sectors[a]
NH2123	*zea-3786*	6	<0.3	76 ± 15	ND[b]
NH2124	*cobU713*	12	0.3	80 ± 14	24
NH2118	*cobP712*	14	0.7	91 ± 2	28
NH2140	*cobP710*	14	0.5	82 ± 9	20
NH2141	*zea-3787*	15	<0.3	29 ± 6	ND
NH2142	*cobJ709*	19	<0.3	53 ± 11	46
NH2119	*cob-708*	28	<0.3	44 ± 10	49
NH2075	*pduF358*	30	0.4	41 ± 16	57
NH2172	*pduC359*	32	<0.3	21 ± 7	43
NH2369	*pdu-360*	36	<0.3	10 ± 8	74
NH2370	*pdu-361*	43	<0.3	10 ± 5	51
NH2453	*zec-8253*	65	<0.3	2 ± 2	79
NH2223	*phs-208*	68	<0.3	25 ± 7	57
NH2149	*hisD10201*	80	<0.3	3 ± 2	85
NH2226	*zee-8251*	90	<0.3	1 ± 1	81

[a] The color of the colony reflects the Lac phenotype (blue = Lac$^+$; white = Lac$^-$).
[b] ND, not determined.

TABLE 4. Characterization of deletion products in stationary-phase (24-h) cultures

Strain	Allele	Deletion size (kb)	Uninduced deletion frequency (%)	Induced deletion frequency (% [mean ± SD])	Fraction of deletions with sectors[a]
NH2123	*zea-3786*	6	<0.1	95 ± 6	ND[b]
NH2124	*cobU713*	12	0.6	99	1
NH2118	*cobP712*	14	3	99	1
NH2140	*cobP710*	14	0.6	96 ± 3	2
NH2141	*zea-3787*	15	<0.1	84 ± 3	ND
NH2142	*cobJ709*	19	1.1	99	2
NH2119	*cob-708*	28	2.2	98	2
NH2075	*pduF358*	30	0.3	71 ± 8	24
NH2172	*pduC359*	32	<0.1	65 ± 28	20
NH2369	*pdu-360*	36	<0.1	46 ± 32	10
NH2370	*pdu-361*	43	0.3	19 ± 8	9
NH2453	*zec-8253*	65	0.4	9 ± 2	28
NH2223	*phs-208*	68	0.4	77 ± 12	14
NH2149	*hisD10201*	80	0.2	9 ± 4	26
NH2226	*zee-8251*	90	<0.1	17 ± 4	23

[a] The color of the colony reflects the Lac phenotype (blue = Lac$^+$; white = Lac$^-$).
[b] ND, not determined.

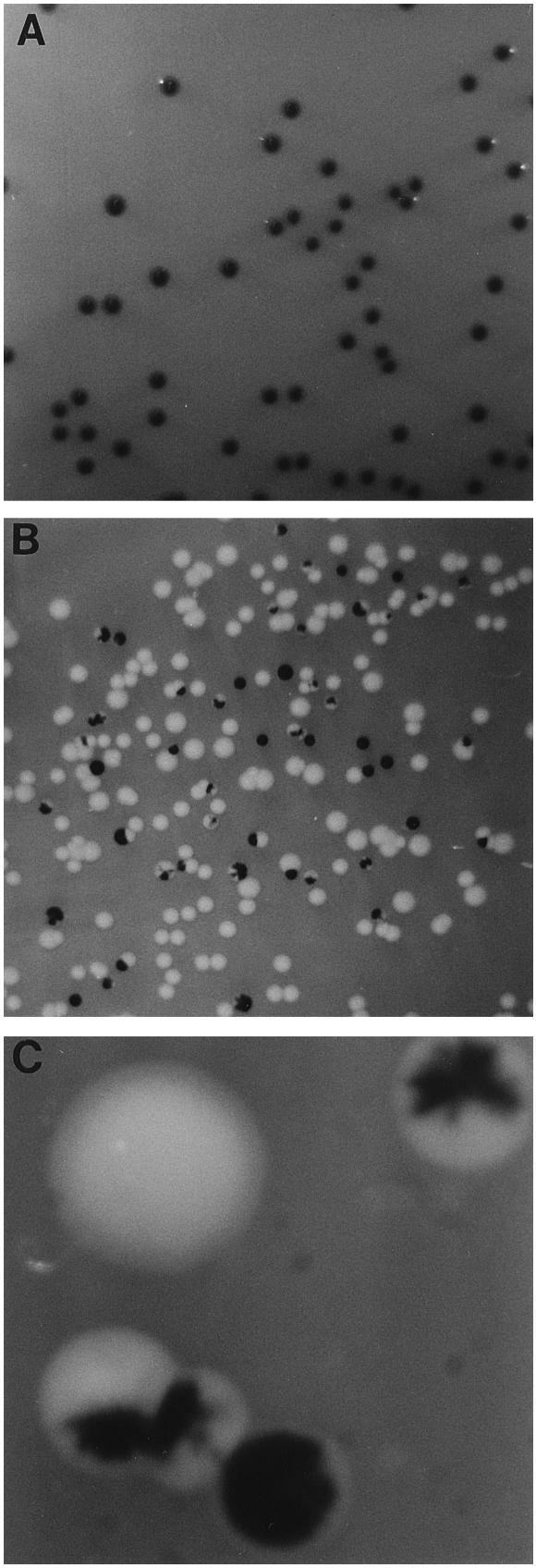

FIG. 5. Colony deletion phenotypes. Cells from strain NH2140 were plated on NCE salts-succinate plates containing X-Gal. (A) Cells from an exponential-phase culture grown to 50 Klett units at 30°C and plated. (B) Cells at 50 Klett units shifted for 10 min to 42°C, shifted back to 30°C, and incubated for 1 h before plating. (C) Enlargement of a cluster of five cells from the center of the field shown in panel B.

in deletion frequency compared with that of the uninduced control population (Tables 3 and 4). Thus, our system meets the second criterion. The assay can be used under different physiological conditions.

Third, to evaluate the variation between cultures, experiments were done in triplicate and a minimum of 500 colonies were analyzed for each strain tested. The standard deviation between three similar cultures differed for different insertions (Table 3). For example, strain NH2140 makes a 14-kb deletion after temperature induction (Fig. 4 and 5). The background frequency of deletions in uninduced cultures was less than 1% (Table 3). After induction, nine independent cultures showed an average colony deletion frequency of 82% with a standard deviation of 20%. Whereas the standard deviation fluctuated for different positions, it was usually a fraction of the measured value. Therefore, this system is reproducible.

Detecting deletions. Variation in growth rate caused some variation in resolution efficiency. Therefore, a protocol was designed to ensure uniform cell growth. On day 1, a strain was streaked onto LB plates containing gentamicin, kanamycin, tetracycline, and chloramphenicol, and plates were incubated at 30°C overnight. On day 2, cells from three well-separated colonies were inoculated into 2-ml liquid cultures of LB medium with 10 μg of gentamicin per ml, 25 μg of kanamycin per ml, 5 μg of tetracycline per ml, and 20 μg of chloramphenicol per ml, and shaking cultures were incubated overnight at 30°C. On day 3, 50-μl aliquots of the overnight cultures were added to 5 ml of sterile LB medium with gentamicin, kanamycin, tetracycline, and chloramphenicol, and these cultures were incubated in 50-ml Nephlo culture flasks (Bellco Glass) in a 30°C shaking water bath. Growth was monitored with a Klett photoelectric colorimeter; when culture turbidity reached a value of 50 Klett units, 1 ml of the culture was removed to a sterile culture tube and the remaining 4 ml of culture was placed at 42°C in a shaking water bath. After 10 min of heat treatment, 20-μl aliquots of the induced culture and the uninduced control were added to 180 μl of LB medium (without drugs) in a microtiter dish and incubated (without shaking) at 30°C for 1 h. Dilutions were made, and cells were spread onto LB or NCE salts-succinate plates containing chloramphenicol and X-Gal.

Deletions extending clockwise (toward *hisD*) were scored for a blue or white color on X-Gal. These deletions remove the expressed *lac* gene present at the left end of the *cobT*::Mu*d*Jr element (Fig. 4). Counterclockwise deletions (toward *supD*) were scored for sensitivity to tetracycline; these deletions eliminate the Tn*10* element inserted just to the right of the *cobT*::Mu*d*Jr element. Of these two methods, the blue or white color phenotype of clockwise deletions was better for two reasons. First, deletions that eliminate *lacZ* expression are easy to visualize, whereas scoring tetracycline sensitivity required inspection of colony replicas plated to two plates. Second, many colonies had both recombinant and nonrecombinant sectors. It was easy to tell a white-sectored colony from a nonrecombinant blue colony but hard to detect sectored colonies after replica plating. In scoring deletions extending to the right, we probably missed some sectored colonies because they had cells that were Tc^r. An example in Fig. 5 shows a field of colonies from a control (Fig. 5A) and induced culture (Fig. 5B) as well

as an enlargement of five colonies from the induced plate (Fig. 5C). Three of the colonies shown in Fig. 5C have obvious white sectors, so we count this field as four colonies with recombinant chromosomes and one blue colony of the nonrecombinant type. In scoring deletions to the right, with the Tc^r instead of the *lac* phenotype, a field of this type would have been scored as two Tc^s recombinants and three Tc^r nonrecombinants. Thus, results involving Tn*10d*Gn elements lying counterclockwise from *cobT* toward the *supD* gene probably underestimate the deletion efficiencies.

Testing resolution over a 2-min segment of *S. typhimurium* chromosome. A survey over a segment of the chromosome that is large enough to include a domain border (>100 kb) showed two striking results. First, resolution reactions were detected between all properly oriented pairs of *res* sites. We found 90-kb deletions in strain NH2226, which involved *cobT714*::Mu*d*Jr2 and *zee-8251*::Tn*10d*Gn, and 15-kb deletions in strain NH2141, which involved *cobT714*::Mu*d*Jr1 and *zea-3787*::Tn*10d*Gn (Table 3; Fig. 4). These two strains demonstrate that *res* site pairing can occur over an interval spanning at least 105 kb of DNA. In addition, all Tn*10d*Gn elements that were located between these two outposts supported resolution when paired with the appropriate Mu*d*Jr element (Table 3). Thus, there was no evidence of a stringent barrier to resolution reactions in the 43- to 45-min region of the genome.

Second, although there were no absolute barriers for resolution, the efficiency of recombination decreased with distance. Sites close together were resolved at frequencies in excess of 80%. The efficiency became progressively lower for sites spaced further apart, reaching a value of 1% in the *zee-8251*::Tn*10d*Gn strain NH2226, which was the most distant insertion tested. This deletion eliminates 90 kb of DNA, and the recombinants had a His^- Phs^- Pdu^- Cob^- Lac^- Gn^r Kn^s Tc^r phenotype, showing that all intervening material was removed.

Segregation and kinetics of deletions. Initially, the RES protein limits recombination. After the induction of RES expression by a heat pulse, another factor that is sensitive to the distance separating *res* sites (supercoil diffusion?) becomes rate limiting until a drop in the RES protein level through dilution or proteolytic digestion again limits the reaction. What is the time frame in which deletions are generated after heat induction of RES protein? At one extreme, RES protein might be active in recombination for only a few moments after its synthesis. Alternatively, RES protein might persist in vivo and remain an active recombinase for a protracted period.

Many deletion-bearing colonies developed multiple white and blue sectors (Fig. 5; Table 3). For example, strain NH2124 generated a 14-kb deletion in which sectored colonies represented 25% of the deletion-bearing clones. The fraction of sectored colonies among total recombinant clones was correlated with interval size. In strain NH2226, which generated a 90-kb deletion, more than 80% of the recombinants were found in sectored colonies (Table 3). This result would be expected if the time frame for recombination was long and the recombination rate for the large deletions was lower than the rate for short intervals.

To examine strand exchange kinetics, resolution was assayed by performing PCR with chromosomal DNA templates. Two strains, NH2124 and NH2119, contain Mu*d*Jr2 and one of two Tn*10d*Gn alleles (*cobU713* or *cob-708*) that make deletions of 12 and 30 kb, respectively. One of the PCR primers matched a sequence within the Tn*10d*Gn element, and the second primer matched a *cob* sequence immediately right (toward *supD*) of the Mu*d*Jr2 insertion point (Fig. 6A). As a positive control, DNA from strain NH2130 was also analyzed; this strain carries the completed deletion that forms in strain NH2119 (Table 1; Fig. 6A). When a chromosomal template from the uninduced parental strain NH2124 or NH2119 was used, the nonrecombinant chromosomal PCR products were too large to detect under standard PCR conditions (17). As expected, both strains generated the same PCR product after deletion formation, i.e.,

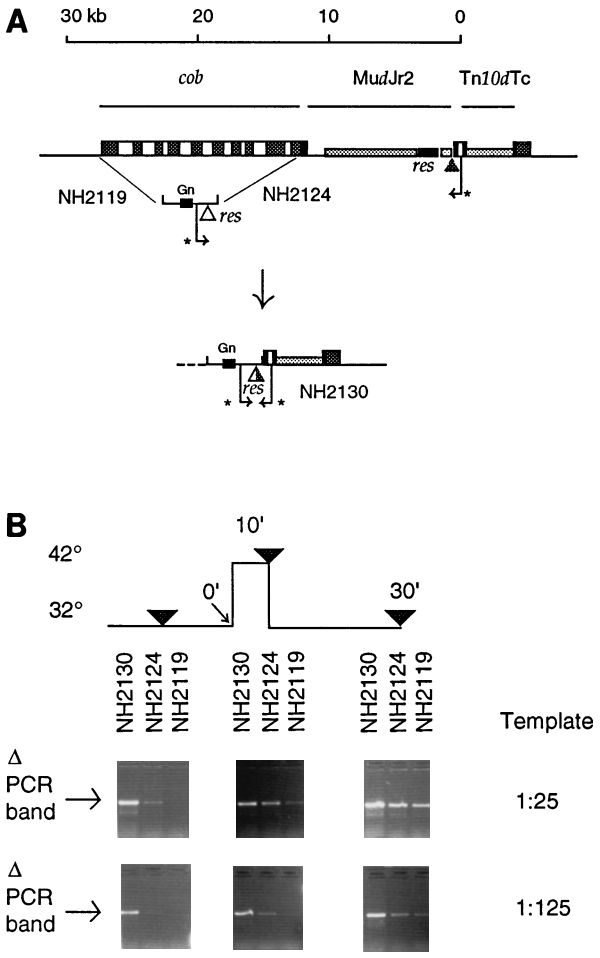

FIG. 6. PCR analysis of two deletions. (A) The physical and genetic map is shown for two deletion intervals that were subjected to PCR analysis. Strains NH2119 and NH2124 have Tn*10d*Gn insertions in the *cobA* and *cobU* genes, respectively. Following RES protein expression, each strain undergoes recombination that deletes the *cob* DNA and Mu*d*Jr2 sequences lying between the *res* sites. Strain NH2130 has the completed deletion that can form in strain NH2119. The deletion products were detected by use of primers matching sequences within the Tn*10d*Gn (GP1) and within a small patch of the *cobT* gene that lies to the right of Mu*d*Jr2 (161OU**I**). The locations of these primer binding sites, which generate a 900-bp band in the deletion product, are shown by arrows flanked with asterisks. (B) Cell cultures were incubated at 30°C in LB medium plus gentamicin, tetracycline, chloramphenicol, and kanamycin. When cultures reached a turbidity corresponding to 50 Klett units, 2-ml aliquots were withdrawn, the cells were concentrated by centrifugation and resuspended in 100 μl of water, and the mixture was heated for 10 min at 94°C. Part of the remaining culture was shifted to 42°C for 10 min, and another 2-ml aliquot was withdrawn, concentrated, and heated to 94°C. The remaining culture was shifted back to 30°C and incubated for 20 min, and then 2 ml was treated as the other two samples were. Each DNA sample was diluted to 1:25 and 1:125 of the original solution in water, and 3 μl of each dilution was added to PCRs with oligonucleotide primers 161OU**I** and GP1. After 30 rounds of thermocycling, each sample was applied to a 1% agarose gel and subjected to electrophoresis. DNA was stained with ethidium bromide and photographed. NH2130 has a 26-kb deletion that eliminates DNA between *cob-708*::Tn*10d*Gn and *cobT714*::Mu*d*Jr2; NH2124 has the *cobU713*::Tn*10d*Gn and yields a 12-kb deletion product; NH2119 has *cob-708*::Tn*10d*Gn and generates the 26-kb deletion present in NH2130. The time line is shown along with the PCR analyses of three strains at times indicated by filled triangles. The position of the 0.9-kb PCR band from chromosomes with deletions is indicated by arrows.

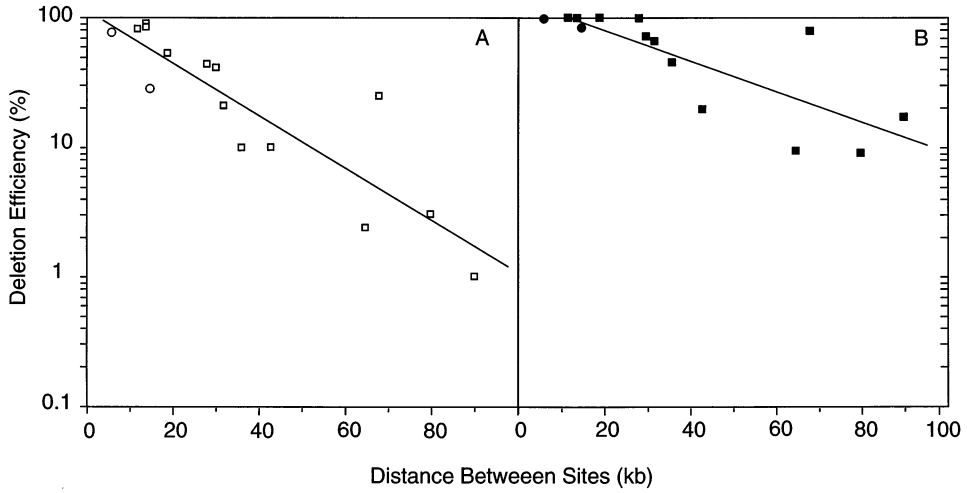

FIG. 7. Relationship between deletion efficiency and distance between *res* sites. The data from Tables 3 and 4 are plotted in semilog format in panels A and B, respectively. The distance between the *res* site in the Tn*10d*Gn element and the *res* site in Mu*dJ* is given along the abscissa in kilobases. Relative to the genetic and physical map in Fig. 3, the clockwise deletions (toward the *his* operon) are represented by squares and the counterclockwise deletions (toward *supD*) are represented by circles. Parameters of the linear plot of deletion frequency (y) versus the distance (x) in panels A and B are, respectively, $y = 120 \cdot 10^{(-0.020x)}$ ($R = 0.9$) and $y = 140 \cdot 10^{(-0.01x)}$ ($R = 0.8$).

a DNA band of 0.9 kb (Fig. 6A). This band was also readily detected in strain NH2130, which carries the completed deletion.

Resolution was fast in some cells (Fig. 6B) and slow in others. For strain NH2124, which has *res* sites separated by 12 kb of intervening DNA, a weak but detectable PCR band was found in the sample taken prior to thermoinduction with the template at a 1:25 dilution. This result agrees with that of the visual plate assay, i.e., 0.3% of uninduced cells from this strain had deletion-bearing chromosomes (Table 3). However, the PCR signal was dramatically stronger by 10 or 30 min after induction. Using the 1:125 dilution of template DNA, NH2124 showed an extremely faint band before induction and bands that increased substantially at the 10- and 30-min time points. For strain NH2119, which generates a 28-kb deletion after RES induction, no PCR products were visible at either template concentration for cells sampled prior to thermoinduction. By 10 min after shifting to 42°C, a 0.9-kb PCR band could be seen in the 1:25 dilution of template DNA, and by 30 min, this band was prominent. At a template dilution of 1:125, DNA from the induced culture of NH2119 showed weaker signals than DNA from the induced culture of NH2124, but a prominent PCR product was visible in reactions using a DNA template isolated 30 min after thermoinduction. As a control, the diagnostic 0.9-kb PCR band was found with both the high (1:125) and low (1:25) dilutions of the template DNA in strain NH2130, which has the completed, characterized deletion (Fig. 6). Although this experiment provides relatively crude quantitation, it shows that some recombination events producing 10- and 28-kb deletions of DNA are complete within 10 min of RES expression. In the two strains tested by PCR analysis, the RES protein remained active for more than 30 min after the induction period. It is likely that some resolution reactions are completed after the time of plating (1 h postinduction).

Resolution reactions in cells at rest (stationary phase). The results described above suggest that topological barriers that limit supercoil diffusion exist, but these barriers seem to be randomly placed. Can a cell change its chromosomal supercoil mobility and thereby alter the efficiency of in vivo recombination? To address this question, we investigated the deletion efficiency after the cells had entered the stationary phase. Samples were withdrawn from cultures incubated for 24 h in LB medium at 30°C, a portion of the culture was placed at 42°C for 10 min, and cells were spread on plates after 1 h of additional incubation at 30°C. Compared with cells tested for deletion formation in the exponential growth phase, there were two significant changes seen for stationary-phase cells. First, deletion frequencies were significantly higher in the stationary-phase cells than they were in exponentially growing cultures; the appearance of the 90-kb deletion in strain NH2226 was more than 10-fold higher in stationary-phase populations (17%) than in exponential-phase cells (1%) (Tables 3 and 4; Fig. 7). Moreover, the deletion frequency increased for all of the DNA segments tested. Second, the segregation patterns were different as well. Resolution of the 14-kb interval (in strains NH2118 and NH2140), which produced 21 to 25% sectored colonies when the experiment was performed on exponential-phase cells, had only 1% sectored colonies when the experiment was done in the stationary phase. In the largest deletion tested (strain NH2226), the number of sectored colonies dropped from over 80% in exponential-phase cells to 23% in stationary-phase cells. Both the increased frequency and diminished sector colony phenotype indicate that a rate-limiting factor is different in stationary-phase cells than in exponentially growing cells. This could be due to the increased persistence or abundance of the RES protein in the stationary-phase cell population or to the elimination in stationary-phase cells of a barrier that interferes with the strand exchange mechanism (i.e., a barrier to supercoil mobility). A test of RES expression using antibodies and Western blot (immunoblot) technology showed that more resolvase was made in exponential-phase cultures than in stationary-phase ones (data not shown). Thus, the increased deletion efficiency seen in stationary-phase populations is highly significant, since it is accomplished with less resolvase than is made in exponential-phase cells.

DISCUSSION

Previous pictures of chromosome domain structure. In the early 1970s, studies on chromosome structure by Worcel and

Burgi (72) and by Pettijohn and Hecht (47) showed that partially condensed supercoiled bodies, or nucleoids, could be isolated from *E. coli* cells. Although the molecular forces that maintained these bodies in a compact structure were largely undefined (47), the behavior of nucleoids suggested the existence of an underlying framework in chromosome architecture. In the mid-1970s, electron micrographs of Kavenoff et al. (33, 34) revealed certain nucleoid preparations to be rosettes of about 50 plectonemically interwound DNA loops (per genome equivalent) emanating from a central core. These pictures reinforced the notion of a chromosomal subgenomic framework. In 1981, Sinden and Pettijohn found in vivo evidence that different supercoiled segments of the *E. coli* chromosome behaved independently (i.e., the chromosome required introduction of multiple nicks to achieve complete relaxation) (59). The experiments of Sinden and Pettijohn provided evidence for in vivo constraints on DNA movements reminiscent of nucleoid behavior; they suggested that a chromosome in a living cell is composed of 50- to 100-kb modular domains.

In 1987, Bliska and Cozzarelli (11) discovered an important detail about supercoil shape. By visually characterizing the in vivo products of bacteriophage λ INT-promoted intramolecular recombination reactions, they showed that plasmid DNA exists largely in the interwound (plectonemically supercoiled) form (11); about half of the linking deficit in their plasmid was captured as interwound catenane nodes of the recombinant molecules, and half of the linking deficit was organized in some nondefined manner. These results were consistent with measurements from other groups, who showed by a variety of methods that half of the negative supercoils in bacterial DNA were under torsional stress while the other half were relieved from strain, perhaps being wrapped on the surface of proteins like RNA polymerase and the histone-like proteins (32, 39, 50, 58, 73). In 1987, a dynamic aspect of genome structure was suggested in the twin supercoiling domain hypothesis of Liu and Wang (37). These authors suggested that processes requiring rapid DNA rotation about an axis (i.e., DNA replication or special cases of RNA transcription) could induce hypernegative supercoiling in one part of the chromosome (behind the transcription or replication machinery) while causing positive supercoiling in another DNA segment (ahead of the machinery) at the same time. This hypothesis accounted for an intimate connection between induced transcription and supercoiling effects seen in vivo on plasmids (27, 48, 49).

Picture of supercoiling in the 43- to 45-min region of *S. typhimurium*. We've studied a segment of the *S. typhimurium* chromosome that, by previous estimates, is large enough to exhibit supercoil domain behavior. γδ *res* sites were arrayed to measure the efficiency of RES-mediated deletions for 15 different segments of the 43- to 45-min region of the chromosome. We found no evidence for a stable framework barrier organizing the chromosome into a sequence-specific 50- to 100-kb DNA domain. In general, distance caused a gradual decline in recombination efficiency (Tables 3 and 4; Fig. 7). When the deletion frequencies of exponentially growing populations (y) were plotted against the distance separating the reacting sites (x), the data fit a curve described by the formula $y = 120 \cdot 10^{(-0.020x)}$. Although more complex curves might fit the data, the correlation coefficient for this equation was good ($R = 0.9$). This equation represents a pseudo-first-order function similar to radioactive decay; the parameter that relates distance to frequency predicts a drop by half for each 17-kb increase in the DNA segment that separates two sites (Fig. 7). Our interpretation of these data is that barriers to supercoil diffusion in the 43- to 45-min region exist, but they are stochastic, varying in position from cell to cell or varying in position within one cell over time (or both).

Local factors undoubtedly influence the γδ resolution recombination efficiency. Among our series of strains, the one that deviates most significantly from the first-order decay curve in Fig. 7 is NH2223. In this strain, a 68-kb deletion occurs at twice the frequency of the 35-kb deletion that occurs in strain NH2369 and 10 times more frequently than its closest neighbor (NH2453). At present, we do not have an explanation for local effects on γδ recombination efficiency. In the homologous (*recA*-dependent) chromosomal recombination pathway, the frequency depends on the position and orientation of *chi* sites (35, 60, 61), and in the phage Mu transposition pathway, insertion efficiency near the *lac* operator is affected by the binding of LacI repressor (68). We anticipate that the types of proteins bound near a resolution sight may affect the interwound structure and there may well be unusual DNA sequences affecting the plectonemic structure of specific DNA regions.

Our system was designed to detect the formation and mobility of interwound (plectonemic) supercoils, which is a necessary precondition for γδ resolution. We suggest that the reduction in deletion frequency seen for distant sites is due to impairment of plectosome formation. Although we cannot eliminate the possibility that segment length limits some other aspect of the reaction, two important points deserve emphasis: (i) no absolute barrier was found (all tested sites were capable of contacting each other in a common plectonemic supercoil); and (ii) supercoiling barriers are plastic and they change with physiology. When stationary-phase cells are compared with exponentially growing populations, deletions in the stationary-phase population occur more efficiently and with less of a segregation lag, leading to sectored clones, in spite of poorer RES expression achieved in the stationary phase. One explanation for these results is that stationary-phase supercoiling is more fluid and therefore more prone to stimulate long-range plectonemic tangling of *res* sites than supercoiling in the chromosomes of exponentially growing populations.

Supercoil diffusion barriers. What factors cause the observed distance-dependent decay of resolution efficiency? Little is known about how distant sites can become interwound in large chromosomes. Two types of displacement of DNA would stimulate the plectonemic pairing of *res* sites spaced far apart—slithering and branching. In the slithering movement, one strand of double helix slides relative to its interwound partner in a serpentine motion. In the branching movement, rotation about a plectonemic coil axis at one position coupled with rotation about a second plectonemic axis can cause winding and unwinding of one strand of double helix about another (Fig. 3B). This motion is reminiscent of branch migration of single strands of DNA in a Holliday junction. If slithering and supercoil branching stimulate *res* site synapsis, then limits on these processes should limit resolution.

Barriers might be generated as a side product of biochemical transactions occurring along the chromosome. One example of an incidental effect would be the anchoring of DNA to a membrane. Lynch and Wang showed that cotranscriptional translation of several different integral membrane proteins could cause hypernegative supercoiling in plasmid DNA (38). During the period when DNA is bound at the membrane, the ability of adjacent DNA sequences to undergo plectonemic branching and slithering might be limited (Fig. 3C). Examples of membrane proteins in the 43- to 45-min interval include the *lacY* gene of Mu*d*J and the tetracycline resistance gene of Tn*10*. There are also known or suspected membrane proteins encoded within the *cob* and *pdu* operons. However, transcrip-

tion of *pdu*, *cob*, and the *cobT714*::Mu*dJ lac* fusion is low under the growth conditions used in our experiments. We know of no highly expressed gene that could cause membrane anchoring in the region between the Mu*dJ res* site and 10 of the Tn*10* elements located within the *cob* or *pdu* operon.

A second type of supercoil barrier that might arise as a collateral side product of gene regulation is a DNA loop. Protein-mediated DNA loops are known to limit DNA synapsis in vitro. Saldanha et al. showed that in a plasmid having three *res* sites, *lacI* repressor binding would impede RES-mediated recombination when a *res* site was isolated within a LacI repression loop (i.e., the *res* site was situated between two *lac* operator sites) (53). The *lac* repressor had no measurable effect on resolution reactions involving a pair of *res* sites lying outside the repression loop (53). Isolation of a *res* site in a stable loop might block supercoil diffusion in vivo and impede RES-mediated recombination with a partner outside the loop. Whereas there are several locations where chromosomal repression loops are thought to exist (1), none are known in the *his-cob-pdu* region.

The movement of interwound supercoils might also be affected by the sequence-specific and nonspecific nucleoid-associated DNA-binding proteins. A group of abundant proteins, which includes HU, IHF, FIS, and H-NS, have been connected to complex chromosomal phenotypes in vivo (24, 26, 42, 55). These proteins interact with many enzymes in DNA replication, recombination, and transcription, and they may stabilize transient DNA loops (references 31 and 66, and see discussion above). It is noteworthy that in the stationary phase, where we have shown the chromosome to be more susceptible to RES-driven deletion reactions, there is a change in the abundance of HU, IHF, FIS, and H-NS proteins (5, 23, 42), and one stationary-phase-specific DNA-binding protein (DPS) is induced (3, 4).

In addition to situations where biochemical transactions stop supercoil movement as an indirect consequence of their reaction mechanism, there may be a requirement for supercoil barriers during DNA replication. For example, Ullsperger et al. have suggested that a barrier to supercoil diffusion might be needed to stop sister chromosomes from becoming tangled together so inextricably that the decatenating enzymes (DNA gyrase and topoisomerase IV) are overwhelmed (65).

Implications. One immediate question raised by our results is what fraction of the bacterial supercoils are stochastically organized like the 43- to 45-min segment of *S. typhimurium* and how much might be ordered more specifically? One large DNA segment demonstrating a periodic supercoil domain organization is bacteriophage Mu. Mu is a temperate virus that becomes an independent topological domain during replicative transposition. To facilitate the interwinding and synapsis of the left and right ends of Mu, which are integrated into host sequences and separated in the linear sequence by 37 kb of DNA, DNA gyrase binds to an extraordinary high-affinity site at the center of the element (43, 45). This gyrase site serves as a symmetry element that stimulates Mu replication (44). Examples of large ordered chromosomal domains in *E. coli* or *S. typhimurium* are unknown. An early report that oxolinic acid treatment of cells could induce cleavage of the *E. coli* chromosome into about 50 fragments (63) has been clouded by experiments using pulsed-field gel electrophoresis, where sequence-specific analysis failed to show evidence for 50 high-affinity gyrase-binding or cleavage sites in the genome (18).

The 43- to 45-min region of the *S. typhimurium* chromosome might be exceptional. The *cob* and *pdu* operons represent a large cluster of genes that were first eliminated and then reintroduced into the *S. typhimurium* genome from a very distantly related organism (36). This DNA segment might lack some regulatory features and control sequences present in the more typical portions of the genome. However, recent studies based on assays designed to detect differences in supercoiling-dependent torsional strain from one region of the chromosome to another gave results consistent with a stochastic chromosome structure. Two groups used supercoiling-dependent promoters to look for region-specific differences in the degree of supercoiling of the bacterial chromosome (40, 46). In both cases, the reporter gene assays showed similar expression levels regardless of the position of the insertion in the bacterial chromosome, indicating a lack of permanent defined boundaries.

If the 43- to 45-min region is typical of a large fraction of the chromosome, then interwound supercoils are a dynamic and mobile facet of chromatin structure. The frequency of the sequence interwinding provides a mechanism to measure point-to-point distance in a chromosome. By binding to one point and "surfing the supercoils," an enzyme could scan a large DNA segment before deciding whether a reaction should or should not be carried out. Interwound structure is used by several enzymes to distinguish between sites on the same chromosome from sites on sister chromosomes and it can also "measure" distance between two sites (Fig. 7). Systems that might exploit such linear information include the homologous *recABCD* recombination machinery (35, 60, 61), DNA mismatch correction enzymes (19), and the intriguing phenomenon of transposition immunity (2, 30, 70).

ACKNOWLEDGMENTS

This work was funded by grants GM33143 (to N.P.H.) and GM34804 (to J.R.R.) from the National Institutes of Health.

We thank T. Bobik, P. Chen, N. R. Cozzarelli, K. Hughes, J. Lawrence, M. Pato, C. Ullsperger, and L. Zechiedrich for advice, unpublished information, oligonucleotide primers, and plasmids; and P. Staczek for providing unpublished data on deletion frequencies.

REFERENCES

1. **Adhya, S.** 1989. Multipartite genetic control elements: communication by DNA loop. Annu. Rev. Genet. **23:**227–250.
2. **Adzuma, K., and K. Mizuuchi.** 1988. Target immunity of Mu transposition reflects a differential distribution of Mu B protein. Cell **53:**257–266.
3. **Almiron, M., A. J. Link, D. Furlong, and R. Kolter.** 1992. A novel DNA-binding protein with regulatory and protective roles in starved *Escherichia coli*. Genes Dev. **6:**2646–2654.
4. **Altuvia, S., M. Almiron, G. Huisman, R. Kolter, and G. Storz.** 1994. The *dps* promoter is activated by OxyR during growth and by IHF and sigma S in stationary phase. Mol. Microbiol. **13:**265–272.
5. **Ball, C., R. Osuna, K. Ferguson, and R. Johnson.** 1992. Dramatic changes in Fis levels upon nutrient upshift in *Escherichia coli*. J. Bacteriol. **174:**8043–8056.
6. **Bender, J., and N. Kleckner.** 1986. Genetic evidence that Tn*10* transposes by a nonreplicative mechanism. Cell **45:**801–815.
7. **Benjamin, H. W., and N. R. Cozzarelli.** 1988. Isolation and characterization of the Tn*3* resolvase synaptic intermediate. EMBO J. **7:**1897–1905.
8. **Benjamin, H. W., M. M. Matzuk, M. A. Krasnow, and N. R. Cozzarelli.** 1985. Recombination site selection by Tn*3* resolvase: topological tests of a tracking mechanism. Cell **40:**147–158.
9. **Berkowitz, D., J. Hushon, H. Whitfield, J. R. Roth, and B. N. Ames.** 1968. Procedure for identifying nonsense mutations. J. Bacteriol. **96:**215–220.
10. **Bliska, J. B., H. W. Benjamin, and N. R. Cozzarelli.** 1991. Mechanism of Tn*3* resolvase recombination in vivo. J. Biol. Chem. **266:**2041–2047.
11. **Bliska, J. B., and N. R. Cozzarelli.** 1987. Use of site-specific recombination as a probe of DNA structure and metabolism in vivo. J. Mol. Biol. **194:**205–218.

11a. **Bobik, T.** Personal communication.

12. **Boocock, M. R., J. S. Brown, and D. J. Sherratt.** 1986. Structural and catalytic properties of specific complexes between Tn*3* resolvase and the recombination site res. Biochem. Soc. Trans. **14:**214–216.
13. **Camilli, A., D. T. Beattie, and J. J. Mekalanos.** 1994. Use of genetic recombination as a reporter for gene expression. Proc. Natl. Acad. Sci. USA **91:**2634–2638.
14. **Casadaban, M. J., and S. N. Cohen.** 1979. Lactose genes fused to exogenous promoters in one step using a Mu-lac bacteriophage: *in vivo* probe for

transcriptional control sequences. Proc. Natl. Acad. Sci. USA **76:**4530–4533.
15. **Castilho, B. A., P. Olfson, and M. J. Casadaban.** 1984. Plasmid insertion mutagenesis and *lac* gene fusion with mini-Mu bacteriophage transposons. J. Bacteriol. **158:**488–495.
16. **Chen, P., M. Alion, N. Weyand, and J. R. Roth.** 1995. The end of the *cob* operon: evidence that the last gene (*cobT*) catalyzes synthesis of the lower ligand of vitamin B_{12}, dimethylbenzimidazole. J. Bacteriol. **177:**1461–1469.
17. **Cheng, S., C. Fockler, W. M. Barnes, and R. Higuchi.** 1994. Effective amplification of long targets from cloned inserts and human genomic DNA. Proc. Natl. Acad. Sci. USA **91:**5695–5699.
18. **Condemine, G., and C. L. Smith.** 1990. Transcription regulates oxolinic acid-induced DNA gyrase cleavage at specific sites on the *E. coli* chromosome. Nucleic Acids Res. **18:**7389–7396.
19. **Cooper, D., R. Lahue, and P. Modrich.** 1993. Methyl-directed mismatch repair is bidirectional. J. Biol. Chem. **268:**11823–11829.
20. **Cozzarelli, N. R., and J. C. Wang.** 1990. DNA topology and its biological effects. Cold Spring Harbor Laboratory, Cold Spring Harbor, N.Y.
21. **Craigie, R., and K. Mizuuchi.** 1986. Role of DNA topology in Mu transposition: mechanism of sensing the relative orientation of two DNA segments. Cell **45:**793–800.
22. **Davis, R. W., D. Botstein, and J. R. Roth.** 1980. A manual for genetic engineering. Advanced bacteria genetics. Cold Spring Harbor Laboratory, Cold Spring Harbor, N.Y.
23. **Dersch, P., K. Schmidt, and E. Bremer.** 1993. Synthesis of the *Escherichia coli* K-12 nucleoid-associated DNA-binding protein H-NS is subjected to growth-phase control and autoregulation. Mol. Microbiol. **8:**875–889.
24. **Drlica, K.** 1992. Control of bacterial supercoiling. Mol. Microbiol. **6:**425–433.
25. **Elliott, T., and J. R. Roth.** 1988. Characterization of Tn*10d*Cam: a transposition defective Tn*10* specifying chloramphenicol resistance. Mol. Gen. Genet. **213:**332–338.
26. **Falconi, M., V. McGovern, C. Gualerzi, D. Hillyard, and N. P. Higgins.** 1991. Mutations altering chromosomal protein H-NS induce mini-Mu transposition. New Biol. **3:**615–625.
27. **Figueroa, N., and L. Bossi.** 1988. Transcription induces gyration of the DNA template in *Escherichia coli*. Proc. Natl. Acad. Sci. USA **85:**9416–9420.
28. **Garrard, W. T.** 1990. Chromosomal loop organization in eukaryotic genomes, p. 163–175. *In* F. Eckstein and D. M. J. Lilley (ed.), Nucleic acids and molecular biology. Springer-Verlag, Berlin.
29. **Gasser, S. M., and U. K. Laemmli.** 1986. Cohabitation of scaffold binding regions with upstream/enhancer elements of three developmentally regulated genes of *D. melanogaster*. Cell **46:**521–530.
30. **Heffron, F.** 1983. Tn*3* and its relatives, p. 223–260. *In* J. A. Shapiro (ed.), Mobile genetic elements. Academic Press, Inc., New York.
31. **Higgins, N. P., D. A. Collier, M. W. Kilpatrick, and H. M. Krause.** 1989. Supercoiling and integration host factor change the DNA conformation and alter the flow of convergent transcription in phage Mu. J. Biol. Chem. **264:**3035–3042.
32. **Jaworski, A., N. P. Higgins, R. D. Wells, and W. Zacharias.** 1991. Topoisomerase mutants and physiological conditions control supercoiling and Z-DNA formation in vivo. J. Biol. Chem. **266:**2576–2581.
33. **Kavenoff, R., and B. Bowen.** 1976. Electron microscopy of membrane-free folded chromosomes from *Escherichia coli*. Chromosoma **59:**89–101.
34. **Kavenoff, R., and O. Ryder.** 1976. Electron microscopy of membrane-associated folded chromosomes of *Escherichia coli*. Chromosoma **55:**13–25.
35. **Kowalczykowski, S. C., D. A. Dixon, A. K. Eggleston, S. D. Lauder, and W. M. Rehrauer.** 1994. Biochemistry of homologous recombination in *Escherichia coli*. Microbiol. Rev. **58:**401–465.
35a. **Lawrence, J.** Unpublished data.
36. **Lawrence, J. G., and J. R. Roth.** 1996. Evolution of coenzyme B_{12} synthesis among enteric bacteria: evidence for loss and reacquisition of a multigene complex. Genetics **142:**11–24.
37. **Liu, L. F., and J. C. Wang.** 1987. Supercoiling of the DNA template during transcription. Proc. Natl. Acad. Sci. USA **84:**7024–7027.
38. **Lynch, A. S., and J. C. Wang.** 1993. Anchoring of DNA to the bacterial cytoplasmic membrane through cotranscriptional synthesis of polypeptides encoding membrane proteins or proteins for export: a mechanism of plasmid hypernegative supercoiling in mutants deficient in DNA topoisomerase I. J. Bacteriol. **175:**1645–1655.
39. **McClellan, J. A., P. Boublikova, E. Palecek, and D. M. J. Lilley.** 1990. Superhelical torsion in cellular DNA responds directly to environmental and genetic factors. Proc. Natl. Acad. Sci. USA **87:**8373–8377.
40. **Miller, W. G., and R. W. Simons.** 1993. Chromosomal supercoiling in *Escherichia coli*. Mol. Microbiol. **10:**675–684.
41. **Morisato, D., J. C. Way, H.-J. Kim, and N. Kleckner.** 1983. Tn*10* transposase acts preferentially on nearby transposon ends in vivo. Cell **32:**799–807.
42. **Nash, H. A.** The *E. coli* HU and IHF proteins: accessory factors for complex protein-DNA assemblies. *In* E. C. C. Lin and A. S. Lynch (ed.), Regulation of gene expression in *Escherichia coli*, in press.
43. **Pato, M., M. M. Howe, and N. P. Higgins.** 1990. A DNA gyrase binding site at the center of the bacteriophage Mu genome required for efficient replicative transposition. Proc. Natl. Acad. Sci. USA **87:**8716–8720.
44. **Pato, M. L., and M. Karlock.** 1994. Central location of the Mu strong gyrase binding site is obligatory for optimal rates of replicative transposition. Proc. Natl. Acad. Sci. USA **91:**7056–7060.
45. **Pato, M. L., M. Karlock, C. Wall, and N. P. Higgins.** 1995. Characterization of Mu prophage lacking the central strong gyrase binding site: location of the block in replication. J. Bacteriol. **177:**5937–5942.
46. **Pavitt, G. D., and C. F. Higgins.** 1993. Chromosomal domains of supercoiling in *Salmonella typhimurium*. Mol. Microbiol. **10:**685–696.
47. **Pettijohn, D. E., and R. Hecht.** 1973. RNA molecules bound to the folded bacterial genome stabilize DNA folds and segregate domains of supercoiling. Cold Spring Harbor Symp. Quant. Biol. **38:**31–41.
48. **Pruss, G. J., and K. Drlica.** 1989. DNA supercoiling and prokaryotic transcription. Cell **56:**521–523.
49. **Pruss, G. J., S. H. Manes, and K. Drlica.** 1982. *Escherichia coli* DNA topoisomerase I mutants: increased supercoiling is corrected by mutations near gyrase genes. Cell **31:**35–42.
50. **Rahmouni, A. R., and R. D. Wells.** 1989. Stabilization of Z DNA in vivo by localized supercoiling. Science **246:**358–363.
51. **Reed, R. R.** 1981. Transposon-mediated site-specific recombination: a defined in vitro system. Cell **25:**713–719.
52. **Roth, R., J. Lawrence, M. Rubenfield, S. Kieffer-Higgins, and G. Church.** 1993. Characterization of the cobalamin (vitamin B_{12}) biosynthetic genes of *Salmonella typhimurium*. J. Bacteriol. **175:**3303–3316.
53. **Saldanha, R., P. Flanagan, and M. Fennewald.** 1987. Recombination by resolvase is inhibited by *lac* repressor simultaneously binding operators between *res* sites. J. Mol. Biol. **196:**505–516.
54. **Sanderson, M. R., P. S. Freemont, P. A. Rice, A. Goldman, G. F. Hatfull, N. D. F. Grindley, and T. A. Steitz.** 1990. The crystal structure of the catalytic domain of the site-specific recombination enzyme γδ resolvase at 2.7 Å resolution. Cell **63:**1323–1329.
55. **Schmid, M. B.** 1988. Structure and function of the bacterial chromosome. Trends Biochem. Sci. **13:**131–135.
56. **Schmieger, H.** 1972. Phage P22 mutants with increased or decreased transduction abilities. Mol. Gen. Genet. **119:**75–88.
57. **Shapiro, J. A.** 1979. Molecular model for the transposition and replication of bacteriophage Mu and other transposable elements. Proc. Natl. Acad. Sci. USA **76:**1933–1937.
58. **Sinden, R. R., J. O. Carlson, and D. E. Pettijohn.** 1980. Torsional tension in the DNA double helix measured with trimethylpsoralen in living *E. coli* cells: analogous measurements in insect and human cells. Cell **21:**773–783.
59. **Sinden, R. R., and D. E. Pettijohn.** 1981. Chromosomes in living *Escherichia coli* cells are segregated into domains of supercoiling. Proc. Natl. Acad. Sci. USA **78:**224–228.
60. **Smith, G. R.** 1989. Homologous recombination in *E. coli*: multiple pathways for multiple reasons. Cell **58:**807–809.
61. **Smith, G. R.** 1991. Conjugational recombination in *E. coli*: myths and mechanisms. Cell **64:**19–27.
62. **Smith, H. O., and M. Levine.** 1967. A phage P22 gene controlling integration of prophage. Virology **31:**207–216.
63. **Snyder, M., and K. Drlica.** 1979. DNA gyrase on the bacterial chromosome: DNA cleavage induced by oxolinic acid. J. Mol. Biol. **131:**287–302.
64. **Stark, M. W., D. J. Sherratt, and M. R. Boocock.** 1989. Site specific recombination by Tn*3* resolvase: topological changes in the forward and reverse reactions. Cell **58:**779–790.
65. **Ullsperger, C. J., A. V. Vologodskii, and N. R. Cozzarelli.** 1995. Unlinking of DNA by toisomerases during DNA replication, p. 115–142. *In* F. Eckstein and D. M. J. Lilley (ed.), Nucleic acids and molecular biology, vol. 9. Springer-Verlag, Berlin.
66. **Vogel, J. L., Z. J. Li, M. M. Howe, A. Toussaint, and N. P. Higgins.** 1991. Temperature-sensitive mutations in the bacteriophage Mu *c* repressor locate a 63-amino-acid DNA-binding domain. J. Bacteriol. **173:**6568–6577.
67. **Voll, M. J., L. A. Cohen, and J. J. Germida.** 1979. *his*-linked hydrogen sulfide locus of *Salmonella typhimurium* and its expression in *Escherichia coli*. J. Bacteriol. **139:**1082–1084.
68. **Wang, X., and N. P. Higgins.** 1994. 'Muprints' of the *lac* operon demonstrate physiological control over the randomness of *in vivo* transposition. Mol. Microbiol. **12:**665–677.
69. **Way, J. C., M. A. Davis, D. Morisato, D. E. Roberts, and N. Kleckner.** 1984. New Tn*10* derivatives for transposon mutagenesis and for construction of *lacZ* operon fusions by transposition. Gene **32:**369–379.
70. **Wiater, L. A., and N. D. F. Grindley.** 1990. Uncoupling of transpositional immunity from γδ transposition by a mutation at the end of γδ. J. Bacteriol. **172:**4959–4963.
71. **Wohlleben, W., W. Arnold, L. Bissonette, A. Palletier, A. Tanguay, P. H. Roy, G. C. Gamboa, G. F. Barry, E. Aubert, J. Davies, and S. A. Kagan.** 1989. On the evolution of Tn*21*-like multiresistance transposons: sequence analysis of the gene (*aacC1*) for gentamicin acetyltransferase-3-I(AAC(3)-I), another member of the Tn*21*-based expression cassette. Mol. Gen. Genet. **217:**202–208.
72. **Worcel, A., and E. Burgi.** 1972. On the structure of the folded chromosome of Escherichia coli. J. Mol. Biol. **71:**127–147.
73. **Zacharias, W., A. Jaworski, J. E. Larson, and R. D. Wells.** 1988. The B- to Z-DNA equilibrium in vivo is perturbed by biological processes. Proc. Natl. Acad. Sci. USA **85:**7069–7073.